Journal of Chromatography B, 878 (2010) 1051–1058

Contents lists available at ScienceDirect

Journal of Chromatography B

journal homepage: www.elsevier.com/locate/chromb

Sedimentation field-flow fractionation separation of proliferative and differentiated subpopulations during Ca^{2+}-induced differentiation in HaCaT cells

Ludovic Micallef[a], Serge Battu[b,*], Aline Pinon[a], Jeanne Cook-Moreau[c], Philippe J.P. Cardot[b], Christiane Delage[a], Alain Simon[a]

[a] Laboratoire de Chimie Physique, EA 4021 "Biomolécules et Thérapies Anti-tumorales", Université de Limoges, Faculté de Pharmacie, 2 rue du Dr Marcland, 87025 Limoges Cedex, France
[b] Laboratoire de Chimie Analytique et Bromatologie, EA 3842, "Homéostasie Cellulaire et Pathologies", Université de Limoges, Faculté de Pharmacie, 2 rue du Docteur Marcland, 87025 Limoges Cedex, France
[c] Laboratoire de Biochimie et de Génétique Moléculaire, EA 4021 "Biomolécules et Thérapies Anti-tumorales", Université de Limoges, Faculté de Pharmacie, 2 rue du Dr Marcland, 87025 Limoges Cedex, France

ARTICLE INFO

Article history:
Received 18 December 2009
Accepted 9 March 2010
Available online 15 March 2010

Keywords:
HaCaT cells
Calcium-induced differentiation
Proliferative activity
Sedimentation field-flow fractionation
Cell sorting

ABSTRACT

The spontaneously immortalized human keratinocyte cell line HaCaT is widely used as a human keratinocyte model. In a previous comparative study between normal human keratinocytes (NHKs) and HaCaT, we reported that Ca^{2+} concentrations greater than 1 mM induced differentiation *in vitro* in both cell types, notably characterized by increased expression of differentiation markers keratins 1 (K1), 10 (K10) and involucrin. Surprisingly, cells had a higher proliferative activity than those cultured with low Ca^{2+} levels. These results raised many questions; in particular concerning the emergence of HaCaT cells subpopulation which would have different differentiation states and/or proliferation rates throughout Ca^{2+}-induced differentiation. To isolate these subpopulations, we used sedimentation field-flow fractionation (SdFFF). Results demonstrated that the most differentiated cells (HC-F1), characterized by the highest expression of keratinocyte differentiation markers, had the lowest proliferative activity. In contrast, less differentiated cells (HC-F2) maintained a higher proliferative activity. SdFFF is a tool to sort differentiated and/or proliferating cells from a total pool previously treated with a Ca^{2+} concentration inducing differentiation, and can be use to prepare biological models necessary for studying HaCaT cell proliferation after Ca^{2+}-induced differentiation treatment.

1. Introduction

In vitro, the normal human keratinocyte (NHK) proliferation–differentiation switch is tightly regulated by extracellular calcium (Ca^{2+}) concentration. Normal human keratinocytes (NHKs) grow optimally when they are cultured in a medium having a Ca^{2+} concentration less than 0.1 mM [1]. Calcium addition (upto 1 mM) to cultures leads to induction of differentiation, correlated with a reduction in cell proliferation and progressive G1 cell cycle arrest [2]. Ca^{2+}-induced differentiation is notably characterized by a series of coordinated morphological changes, such as stratification and desmosome formation [3,4]. These events are coupled with the expression of keratins 1 (K1) and 10 (K10), the earliest markers of terminal differentiation [5,6] principally localized in the upper layers of spinous cells [7], subsequently followed by increased expression of involucrin [8], localized in the lowest layers of spinous cells as well as in the granular layer [9,10].

As NHKs cultured in an appropriate medium provide an ideal experimental system to study mechanisms implicated in the growth-differentiation switch *in vitro*, their use can be limited due to the complexities involved in their cultivation, recovery from donors, low number of passages, due to their restricted number of cellular divisions, and fibroblast co-culture. The use of a cell line such as the spontaneously immortalized keratinocyte cell line HaCaT would overcome these inconveniences. It has been reported that the HaCaT cell line was able to differentiate and form a stratified epidermal structure [11]. Like NHKs, when HaCaT cells were cultured in low calcium (LC, <0.1 mM) medium, differentiation was induced with confluence state [12–15]. It was also demonstrated that HaCaT cells, cultured in a keratinocyte serum free medium containing high calcium (HC, 1.2 mM) concentration, had a high rate of proliferation, compared to cells cultured with low calcium (optimal culture conditions: LC, 0.09 mM) [14,16]. On the other hand, in high calcium medium-cultured HaCaT cells (HC), this increased

* Corresponding author. Tel.: +33 5 5543 5979; fax: +33 5 5543 5858.
E-mail address: serge.battu@unilim.fr (S. Battu).

1570-0232/$ – see front matter © 2010 Elsevier B.V. All rights reserved.
doi:10.1016/j.jchromb.2010.03.009

proliferation did not prevent differentiation, as shown by an increase in K1, K10 and involucrin expression [14]. These results appeared surprising and raised the following questions: (1) how could Ca^{2+}-induced differentiation be associated with a proliferative activity higher than in LC conditions? (2) In this particular context, was it possible that differentiated cells continued to proliferate when logically, differentiated cells lose this ability? Could this be due to the emergence of several sub-cellular populations throughout Ca^{2+}-induced differentiation? In this paper, we wanted to determine whether several sub-cellular populations existed, in order to confirm if proliferative activity could be attributed to differentiated or undifferentiated cells.

Cell separation methods play an increasing role in many domains such as cell biology, molecular genetics, cellular therapies or clinical diagnostics [17–24]. Sedimentation field-flow fractionation (SdFFF) is a gentle, non-invasive and tagless method. These advantages are based on the drastic limitation of cell-solid phase interaction by the use of (1) a specific separation device: empty ribbon-like channel without stationary phase; and (2) a device setup allowing the "Hyperlayer" elution mode, a size/density driven separation mechanism. As are many other cell separation techniques (elutriation, microfluidic devices, ...), the principle of cell separation is based on physical criteria (size and density) [17,18,20,22,25], depending to the differential elution of species submitted to the combined action of (1) a parabolic profile generated by flowing a mobile phase through a ribbon-like capillary channel; and (2) an external field applied perpendicularly to the flow direction [26,27]. In SdFFF, a multi-gravitational external field is generated by rotation of the separation channel in a rotor basket, constituting one of the most complex devices used in FFF separation [17,27,28]. Since the report of Caldwell et al. [29] on mammalian cells, FFF, SdFFF and related technologies have been used in many biological fields such as hematology, microorganism analysis, biotechnology, molecular biology, neurology and cancer research [18,30–39]. Over several years, we used SdFFF in cancer research to study chemical induced apoptosis or differentiation in cancer cell lines. Different aspects have been evaluated including (1) monitoring of biological events [40–43]; (2) cell sorting of specific subpopulations such as pre-apoptotic [43], or differentiated cells [41]; (3) kinetics of biological events using both the monitoring and cell separation capacities of SdFFF [44,45]; and (4) cell sorting of specific phenotypes from complex cancer cell populations such as neuroblastomas [46,47]. Recently, we also used SdFFF to better understand the possible link between the kinetics and the extent of a biological event, such as apoptosis, and cell status (cell cycle position) at the start of induction [48].

The aim of this study was to determine the correlation between Ca^{2+}-induced differentiation (HC cells), and the surprising increase in proliferative activity. To achieve this goal, we had to sort the different subpopulations in order to (1) characterize their differentiation stage, and (2) determine proliferative activity. To do this, SdFFF was preliminarily used as a cell sorter. As we already reported that K1 and K10 expression increased significantly from day 3, whereas involucrin expression increased from day 6 in HaCaT cells cultured with 1.2 mM Ca^{2+} [14], we chose to cultivate HaCaT cells for 7 days before SdFFF elution. Afterwards, differentiation was determined by measuring the expression of specific differentiation markers K1, K10 and involucrin, by semi-quantitative RT-PCR. Size distribution, proliferative activity, as well as cell cycle position were also studied on the different fractions obtained after SdFFF sorting.

Results showed that SdFFF was able to take into account the variation in size/density balance throughout Ca^{2+}-induced differentiation of HaCaT cells, resulting in the isolation of a differentiated subpopulation having a lower proliferative activity from a less differentiated subpopulation having a higher rate of proliferation.

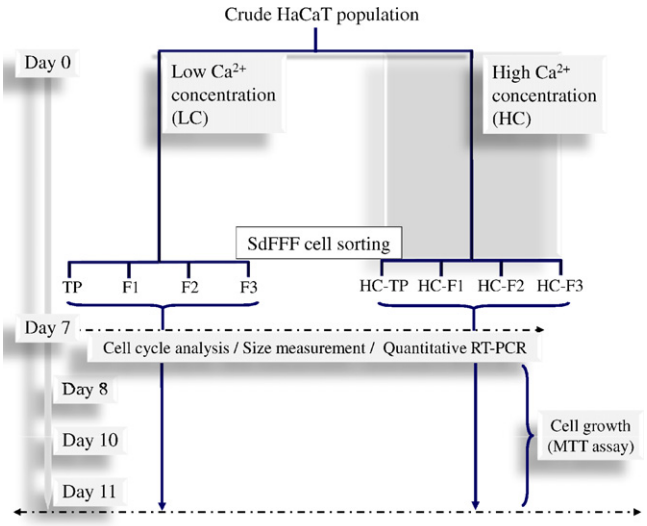

Fig. 1. Preparation of different HaCaT cell subpopulations, ranging from LC (control: low Ca^{2+} level) to HC (treated cells: high Ca^{2+} level). After 7 days culture, cells were eluted by SdFFF and fractions analyzed for expression of differentiation markers, cycle stage and size distribution. Fractions were also subcultured (24, 72 and 96 h) to measure proliferative activity (MTT assay).

2. Materials and methods

2.1. Cell culture

The spontaneously immortalized human keratinocyte cell line HaCaT was cultured in Keratinocyte Serum Free Medium (KSFM, Gibco, Cergy Pontoise, France) already containing 0.09 mM Ca^{2+}, supplemented with 25 μg/mL bovine pituitary extract (BPE, Gibco), 1.5 ng/mL of recombinant epidermal growth factor (rEGF, Gibco), 100 U/mL of penicillin and 100 μg/mL of streptomycin (Gibco). HaCaT cells were maintained in a humidified 5% CO_2 atmosphere at 37 °C. Before SdFFF experiments, freshly trypsinized HaCaT cells were seeded at a density of 3×10^4 cells/cm^2. After 24 h adhesion, medium was removed and replaced by fresh medium. To induce differentiation, cells were cultured during 7 days either with high Ca^{2+} KSFM (HC, 1.2 mM Ca^{2+}) or with low Ca^{2+} KSFM (LC, 0.09 mM Ca^{2+}) (Fig. 1). In LC, differentiation is induced by confluence state.

2.2. SdFFF device, cell elution conditions and subpopulation preparation

The SdFFF separation device used in this study derived from those previously described and schematized [43,45]. The apparatus was composed of two 880 mm × 66 mm × 2 mm polystyrene plates, separated by a Mylar® spacer in which the channel was carved. Channel dimensions were 781 mm × 10 mm × 0.125 mm with two 70 mm V-shaped ends. The measured total void volume (channel volume + connecting tubing + injection and detection device) was 1123 ± 2 μL (n = 6). Void volume was calculated after injection and retention time determination of a non-retained compound (0.10 g/L of benzoic acid, UV detection at 254 nm). The channel rotor axis distance was measured at r = 13.80 cm. A Waters 515 programmable HPLC pump (Waters Associates, Milford, MA, USA) was used to pump the sterile mobile phase. Samples were injected by means of a Rheodyne® 7125i chromatographic injector (Rheodyne®, Cotati, CA, USA). The elution signal was recorded at 254 nm by a Waters 486 Tunable Absorbance Detector (Waters Associates) and a M1111 (100 mV input) acquisition system (Keithley, Metrabyte, Tauton, MA, USA) operated at 4 Hz connected to a PC

computer. A M71B4 Carpanelli engine (Bologna, Italy) coupled to a Mininvert 370 pilot unit (Richard Systems, Les Ullis, France) controlled the rotating speed of the centrifuge baskets. Sedimentation fields were expressed in units of gravity, $1g = 980\,cm/s^2$, and calculated as previously described [36]. Cleaning and decontamination procedures have been previously described [17].

The optimal elution conditions ("Hyperlayer" mode) were determined experimentally and were: flow injection through the accumulation wall of 100 μL HaCaT cell suspension (2.5×10^6 cells/mL); flow rate: 0.80 mL/min; mobile phase: sterile PBS (phosphate buffered solution), pH 7.4 (Gibco); external multi-gravitational field strength: $30.00 \pm 0.01g$ (441.0 ± 0.1 rpm).

Fig. 1 summarizes the protocol used to prepare the different studied subpopulations. After 7 days incubation with low (LC or control cells) or high (HC or treated cells) Ca^{2+} concentration, HaCaT cells (2.5×10^6 cells/mL in sterile PBS pH 7.4) were eluted resulting in the separation of four cell fractions collected and designated as follows (1) TP for total peak; and (2) Fn for fraction number with F1, F2 and F3. Fraction collection was done for LC as follows: TP: 2–5 min/F1: 2–3 min 20 s/F2: 3 min 20 s to 4 min/F3: 4–5 min (Fig. 2A). Fraction collection was done for HC as follows: HC-TP: 2–5 min/HC-F1: 2 min to 3 min 10 s/HC-F2: 3 min 10 s to 3 min 50 s/HC-F3: 3 min 50 s to 5 min (Fig. 2B). To obtain a sufficient quantity of cells for cell cycle studies, size distribution analysis, culture and proliferative activity studies, or for quantitative RT-PCR (Fig. 1), successive SdFFF cumulative fraction collections were performed (10–14).

2.3. Real-time semi-quantitative reverse-transcription-PCR

Cells were cultured during 7 days either with (1.2 mM) or without (0.09 mM) Ca^{2+} addition before being fractionated by SdFFF (Fig. 1). Next, total RNA was extracted from each sample by using the PureLink™ Micro-to-Midi Total RNA Purification System (Invitrogen, Cergy Pontoise, France), according to the manufacturer's instructions. The integrity of total mRNA extracted was evaluated with 1% agarose gel electrophoresis and quantified spectrophotometrically. Total RNA (1 μg) was reverse-transcribed with SuperScript™ Reverse Transcriptase (Invitrogen). Resulting cDNAs were analyzed by using the Rotor-Gene 6000 (LABGENE Scientific Instruments, Archamps, France) and SYBR Green SensiMix dT mix (Quantace, London, England) according to the manufacturer's instructions. Briefly, the reaction mixture containing cDNA, SYBR Green and primer mix (300 nM) was placed in each reaction tube. The reaction conditions were set at 95 °C for 3 min followed by 40 cycles at 95 °C for 15 s and 60 °C for 30 s. Specific primers were designed for qPCR with Beacon Designer software (Bio-Rad, Hercules, CA, USA, Table 1) and their efficiency was calculated by using cDNA dilution curves and linear regression.

None of the primer sequences showed genomic cross reactivity with other genes in a BLAST search analysis (NCBI, http://www.ncbi.nlm.nih.gov/BLAST/). The cycle threshold (Ct) values of the gene of interest (gi) were correlated to the amount of targeted mRNA. For normalization, one housekeeping gene (hg) was chosen among D-glyceraldehyde-3-phosphate dehydrogenase

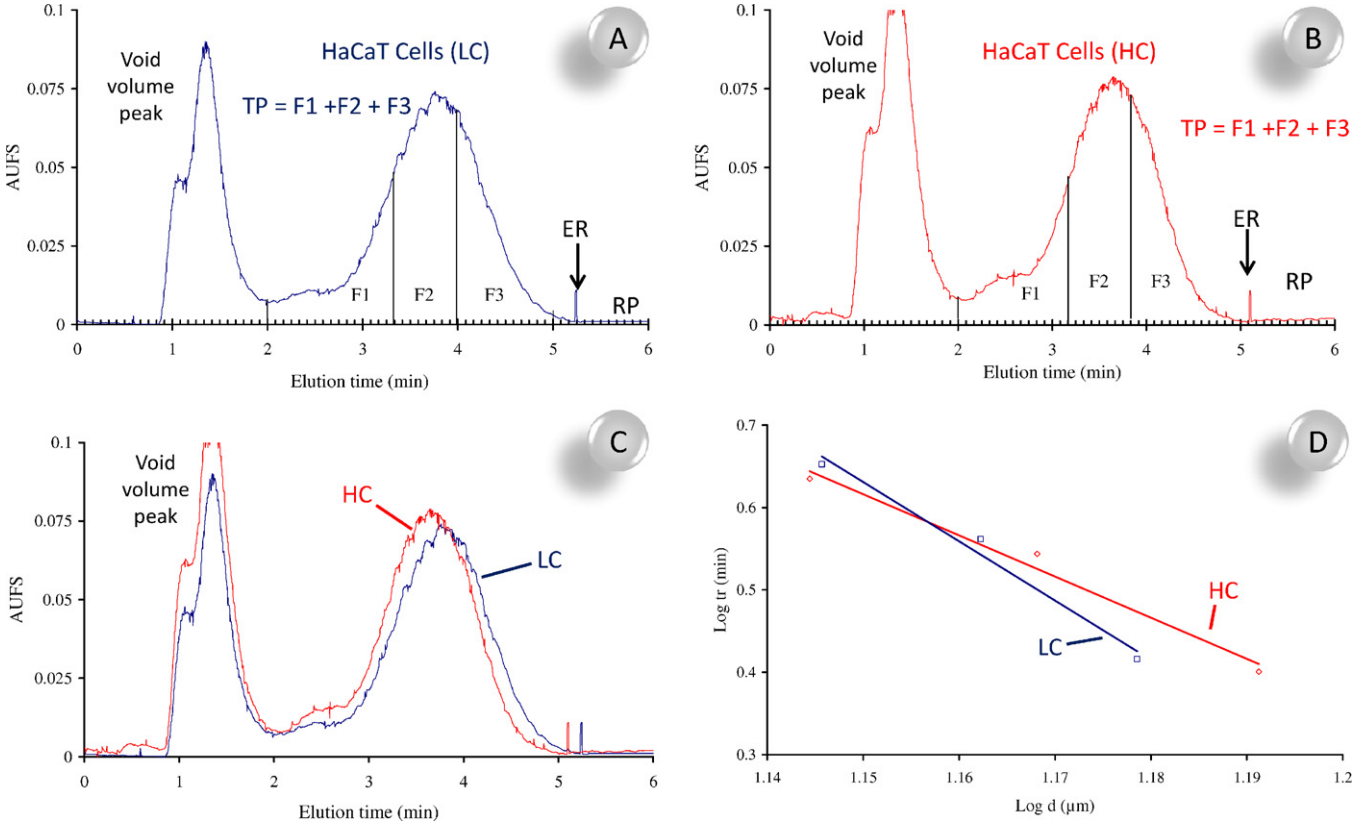

Fig. 2. Representative fractograms of HaCaT cells and fraction collection. (A) LC cells; (B) HC cells; (C) superposition of LC and HC profiles; (D) experimental SdFFF size selectivity curve for control and treated cells. Data points are provided from three independent SdFFF elution for concordant LC and HC cells. Fraction collections were performed as described below. The mean t_R was used to calculate $\log t_R$. The mean cell diameter, measured by Coulter Counter, was used to calculate $\log d$. Experimental data are shown with linear regression curve which was used to calculate the slope of the curve—S_d, where S_d (S_{dObs}) is the size selectivity coefficient. Elution conditions: flow injection of 100 μL cell suspension (2.5×10^6 cells/mL), flow rate: 0.8 mL/min (sterile PBS, pH 7.4); external multi-gravitational field: $30.00 \pm 0.01g$, spectrophotometric detection at $\lambda = 254$ nm. ER corresponds to the end of channel rotation (mean externally field strength = 0g). RP: residual signal corresponding to the release peak of reversible cell-accumulation wall sticking. Fraction collection: (A) TP: 2–5 min (TP = F1 + F2 + F3)/F1: 2–3 min 20 s/F2: 3 min 20 s to 4 min/F3: 4 min to 5 min. (B) HC-TP: 2–5 min/HC-F1: 2–3 min 10 s/HC-F2: 3 min 10 s to 3 min 50 s/HC-F3: 3 min 50 s to 5 min.

Table 1
Expression of terminal differentiation markers at the mRNA level in NHK and in HaCaT cells. The SyBR Green primer sequences (FP forward, RP reverse) used in specific semi-quantitative reverse-transcription/polymerase chain reactions for K1, K10, involucrin and hypoxanthine phosphoribosyl transferase (HPRT) were designed with Beacon Designer software (Biorad). D-Glyceraldehyde-3-phosphate dehydrogenase primers were as described in [14].

Marker	Primer pair	GenBank accession number
K1	FP: 5′ ATTTCTGAGCTGAATCGTGTGATC 3′ RP: 5′ CTTGGCATCCTTGAGGGCATT3′	BC063697
K10	FP: 5′ TGATGTGAATGTGGAAATGAATGC 3′ RP: 5′ GTAGTCAGTTCCTTGCTCTTTTCA 3′	NM_000421
Involucrin	FP: 5′ GGGTGGTTATTTATGTTTGGGTGG 3′ RP: 5′ GCCAGGTCCAAGACATTCAAC 3′	BC046391
HPRT	FP: 5′ GGACAGGACTGAACGTCTTGCT 3′ RP: 5′AAAGAATTTATAGCCCCCCTTGA 3′	NM_000194
GAPDH	FP: 5′ TGCACCACCAACTGCTTAGC 3′ RP: 5′ GGCATGGACTGTGGTCATGAG 3′	BC020308
UBC	FP: 5′ ATTTGGGTCGCGGTTCTTG 3′ RP: 5′ TGCCTTGACATTCTCGATGGT 3′	M26880

(GAPDH), hypoxanthine phosphoribosyl transferase (HPRT) and Human ubiquitin (UBC) and amplified in the same assay, after Ct processing with a geNorm algorithm [49]. The Ct(hg) value was substracted from the Ct(gi) value to give rise to ΔCt, which represented the relative amount of gi transcripts. The fold increase was then calculated as $2^{-\Delta\Delta Ct}$, by comparing each sample *vs*. reference from the ΔΔCt value (ΔCtgi[sample] − ΔCtgi[control]). Reference corresponded to HC-TP.

2.4. Proliferative activity assay

To evaluate proliferative activity of the different fractions, the MTT colorimetric assay was performed as described by Mosmann [50]. This test is based on the selective ability of cells which conserve a metabolic activity to reduce the yellow salt MTT [3-(4,5-dimethylthiazol-2-yl-2,5-diphenyltetrazoliumbromide)] (Sigma, Saint-Quentin Fallavier, France) to a purple–blue insoluble formazan precipitate. MTT was dissolved in PBS at 5 mg/mL. Experiments were performed in 100 μL medium in 96-well plates.

Briefly, cells were cultured during 7 days either with (1.2 mM) or without (0.09 mM) Ca^{2+} addition before being fractionated by SdFFF (Fig. 1). Afterwards, each fraction containing cells was counted by the trypan blue dye exclusion method before being strictly seeded at the same density (3×10^3 cells/well) for further proliferative activity comparisons. After 24, 72, and 96 h incubation, stock MTT solution (10/100 μL medium) was added and plates were incubated at 37 °C for 4 h (Fig. 1). Then, 100 μL sodium dodecyl sulfate (SDS; Sigma; 10% in 0.01 M HCl) was added to each well and the amount of formazan formed was obtained by scanning with an ELISA reader at 550 nm. Six wells per dose and time point were counted in the different experiments.

2.5. Analysis of DNA content by flow cytometry

Cells were cultured during 7 days either with (1.2 mM) or without (0.09 mM) Ca^{2+} addition before being fractionated by SdFFF (Fig. 1). Then, each cell sample was fixed in 1 mL cold 70% ethanol in PBS, washed in PBS and stained with Propidium Iodide (PI, 50 μg/mL final concentration). Flow cytometric analyses were performed as previously described [51] using a FACS Vantage cell sorter (Becton-Dickinson, San Jose, CA) equipped with a 488 nm argon laser. For each sample, the forward *vs*. right-angle scatter cytogram was used to exclude debris and aggregates. A minimum of 2×10^4 cells were analyzed with linear amplification for PI fluorescence that was collected with a 600 nm long pass filter. Cell distribution in the different phases of the cell cycle was estimated using ModFit LT™ (Verity Software House, Inc., Topsham, ME).

2.6. Coulter Counter

A 256 channel Multisizer II Coulter Counter (Beckman Coulter, Fullerton, CA) was used to determine the mean cell population diameter. Cells: crude population or SdFFF collected fraction were diluted in Isoton® to a final volume of 15 mL. The counting conditions were 500 μL sample volume, cumulating three successive assays. Results are displayed as the mean ± SD.

2.7. Statistical analysis

The medians and standard deviations (SD) were calculated using Excel software (Microsoft, Version 2002). Statistical analyses (Statview, Version 5.0) of differences between fractions were carried out by ANOVA test. For real-time semi-quantitative reverse-transcription-PCR experiments, significance was calculated from ΔCt values. Standard deviations were calculated as described above [14]. Both parameters are given on graphs illustrating a "rate of expression". Asterisks correspond to *p*-values of LC TP, F1, F2 and F3 *vs*. HC TP. $^{*}p < 0.05$; $^{**}p < 0.01$; $^{***}p < 0.001$. A value of $p < 0.05$ was considered statistically significant.

3. Results and discussion

3.1. SdFFF cell elution and fraction collection

As previously described [17,47,52], the elution mode of cells is described as "Hyperlayer", a size/density dependent cell elution mode [27,29,53–57], which predicts that large and weaker cells are focused in faster streamlines to be eluted first. Cells are focused in a thin layer away from the accumulation wall enhancing subpopulation sorting and reducing cell-accumulation wall interactions. Hyperlayer elution allowed cell sorting taking into account many specific considerations such as (1) respect of cell functional integrity; (2) providing a high level of short and long term cell viability without induction of apoptosis; (3) not altering the maturation and differentiation stages of eluted cells; and (4) providing high repeatability, reproducibility and recovery. Device setup, elution conditions, as well as cleaning and decontamination procedures [17] were optimized to enhance the "Hyperlayer" elution mode. The different average velocities, and the retention order of different species were compared by means of the observed retention ratio R_{obs} (retention ratio R_{obs} = void time *vs*. retention time = t_0/t_R [57,58]).

Fig. 2A–C displays representative fractograms of HaCaT cells which consisted of two peaks, the first corresponding to the void volume peak ($R_{obs} \approx 1$). The void volume was essentially due to the UV absorbance of components such as residual trypsinization and culture medium, cell fragments, proteins or organelles which were not retained. Nevertheless, the use of flow injection process lead to the presence of few cells [17]. The second corresponding to the cell species with $R_{obs} = 0.374 \pm 0.015$ ($n > 15$) for LC (Fig. 2A) and $R_{obs} = 0.396 \pm 0.016$ ($n > 15$) for treated cells (Fig. 2B). As previously described [4,6,7,10,18,25,39], the external field and flow rate dependence of R_{obs} is one of the most important parameters to confirm the "Hyperlayer" elution mode. The R_{obs} values depend on conditions and culture time [42]. Results displayed in Table 2 demonstrated the external field and flow rate dependence of R_{obs} for LC and HC populations. Besides the field or flow dependence of R_{obs}, the "Hyperlayer" elution mode description also predicted that

Table 2
Variation of the retention ratio R_{obs} of HaCaT cells. Elution conditions: flow injection of 100 μL HaCaT cells (2.5×10^6 cells/mL), mobile phase: sterile PBS pH 7, spectrophotometric detection at λ = 254 nm. Results were expressed as mean ± SD for $n = 3$ (independent SdFFF injection).

	External field		
	20*g*	30*g*	40*g*
	Flow rate (mL/min)		
	1.0	0.8	0.6
LC	0.603 ± 0.012	0.374 ± 0.015	0.251 ± 0.013
HC	0.604 ± 0.013	0.396 ± 0.016	0.254 ± 0.015

samples were not in close contact with the accumulation wall. By using the following equation [40,42,53],

$$R = \frac{6s}{\omega} \quad (1)$$

where R is the retention ratio, ω is the channel thickness (125 μm), and s the distance of the center of the focused zone from the channel wall [53], we calculated the approximate average cell elevation (s) using R_{obs} values. The LC and HC average s were respectively 7.80 and 8.25 μm. The mean cell diameter was 14.67 ± 0.15 μm (control), and 14.90 ± 0.15 μm for treated cells ($n = 6$, Coulter Counter). Thus, as cell radii (a) were less than s: 7.33 < 7.80 μm (LC) −7.45 < 8.25 μm (HC); the HaCaT cell "Hyperlayer" elution was confirmed.

As described above, "Hyperlayer" elution reduced harmful cell/accumulation wall interactions which was demonstrated in part by the low level of the corresponding cell release peak observed at the end of fractogram (RP, Fig. 2A and B), when the external field was turned off (ER: mean external field = 0.00*g*).

As widely described [40–44,59], a shift in R_{obs} between control and treated cells is a proof of biological event induction. In the case of Ca^{2+}-induced differentiation of HaCaT cells, we observed only a slight shifting of R_{obs} values in comparison to that of observed for HEL (human erythroleukemia cell line) cells for which we observe that R_{obs} increase from 0.353 to 0.395 only after 24 h incubation with diosgenin [44]. After 96 h incubation the difference between R_{obs} reached 0.100 units [41]. Thus, in the case of HaCaT cells only a small size increase was observed, leading to minor changes in R_{obs} (Fig. 2C).

Then, we analyzed the change of the size/density balance ratio throughout differentiation. As previously described [41,43,60], size selectivity was experimentally established, by using the following equation [61]:

$$\log\ t_r = -S_d \log d + \log t_{R1} \quad (2)$$

where $-S_d$, the slope of the graph, represents the selectivity coefficient; t_r is the retention time, d the mean cell diameter and t_{R1} a constant value, equal to the retention time of a 1 μm particle. It has been demonstrated [61] that in the case of elution of a population containing particles of different sizes, but analogous density profiles, the size selectivity curve is a straight line. As previously described [41,43,60], by using fraction collection (Fig. 2A and B) and the Coulter Counter, we established experimental size selectivity curves (Fig. 2D) in order to calculate an observed S_d value: S_{dObs}, which could be used to compare different devices, elution conditions, or to compare the impact of biological event induction on the size/density equilibrium [41,43].

In the case of LC cells, the size selectivity curve was a straight line ($r = 0.991$), allowing the calculation of a high $S_{dObs} = 7.18$ ($n = 3$). For HC cells the size selectivity curve was also a straight line ($r = 0.991$), giving $S_{dObs} = 5.00$ ($n = 3$) (Fig. 2D). S_{dObs} is defined as the slope of the graph given by Eq. (3),

$$S_d = \left| \frac{d\log(t_r)}{d\log(d)} \right| \quad (3)$$

The difference between these populations was essentially linked to the $d\log(d)$, where the difference in diameter between the beginning and end of the fractogram was ≈1.60 μm for HC cells, reducing S_{dObs}, and only ≈1.00 μm for LC. Principal differences specifically concerned F1, with an increase of ≈0.5–0.6 μm in diameter for HC cells compared to LC, while F2 and F3 did not have significant difference in size (Fig. 2D). Therefore, the effect of differentiation on the size/density balance ratio seemed to concern essentially F1 of HC cells.

In light of the results concerning (1) R_{obs} field and flow dependence; (2) $s > a$; (3) the linear size selectivity curve and high value for S_{dObs}; and finally (4) low levels of reversible cell release (Fig. 2A–C); we could assume that HaCaT cells eluted under the "Hyperlayer" mode.

From a biophysical point of view, SdFFF takes into account the change in the size/density balance induced by Ca^{2+} treatment. As shown in Fig. 2B, four cell fractions were collected from HC population (1) the total peak fraction (TP) which corresponded to the total HaCaT population eluted; and (2) peak fractions 1, 2 and 3 (HC-Fn) which are the time-dependent collected fractions of the retained peak profile.

Cell differentiation marker expression, proliferative activity and cell cycle analysis were conducted both on SdFFF eluted fractions and on crude populations (Fig. 1) in order to determine whether SdFFF enhanced separation of a population of interest, in particular if we were able to sort cells with different maturation stages and if they expressed differences in proliferative activities.

3.2. Fraction characterization

3.2.1. Semi-quantitative RT-PCR

Semi-quantitative RT-PCR was used to measure mRNA levels of K1, K10, and involucrin in HaCaT cells after SdFFF [14]. Keratin genes code for intermediate filament proteins. K1 and K10 form a differentiation-specific keratin pair. When basal keratinocytes become committed to terminal differentiation, they stop dividing and move into the suprabasal compartment. They then express K1 and K10 as the predominant keratin pair [7]. The involucrin gene codes for a precursor protein of the cornified envelope, synthesized in cells of the upper spinous and granular layers. In HaCaT cells cultured with 1.2 mM Ca^{2+}, K1 and K10 expression increased significantly from day 3, whereas involucrin expression increased from day 6. In HaCaT cells cultured without Ca^{2+} addition (0.09 mM) and with the same seeding density as HC (3×10^4 cells/cm^2), K1, K10 and involucrin expression increased at day 6, in agreement with confluence state [14]. These preliminary results led us to cultivate HaCaT cells for 7 days at various Ca^{2+} concentrations before using SdFFF to sort cells and consequently to analyze differentiation markers expression in the different fractions obtained.

For all experiments, results are reported by comparing mRNA expression of each sample (LC-TP, HC-F1, HC-F2 and HC-F3) *vs.* HC-TP, which was considered as the reference (Fig. 3). For all differentiation markers, we systematically observed a lower expression in LC-TP, compared with HC-TP (Fig. 3), despite the fact that LC cultured cells reached confluence. This result confirmed that SdFFF cell elution did not alter expression of differentiation markers such as K1, K10 and involucrin in HC cells. Using SdFFF, HC cells were then separated in three fractions: HC-F1, -F2 and -F3 (Figs. 1 and 2). Results demonstrated that HC-F1 systematically showed the highest level of transcripts, compared with HC-F2 and HC-F3. Moreover, HC-F1 expressed a higher level of K10 and involucrin than HC-TP. In HC-F2 and HC-F3, differentiation marker expression was lower

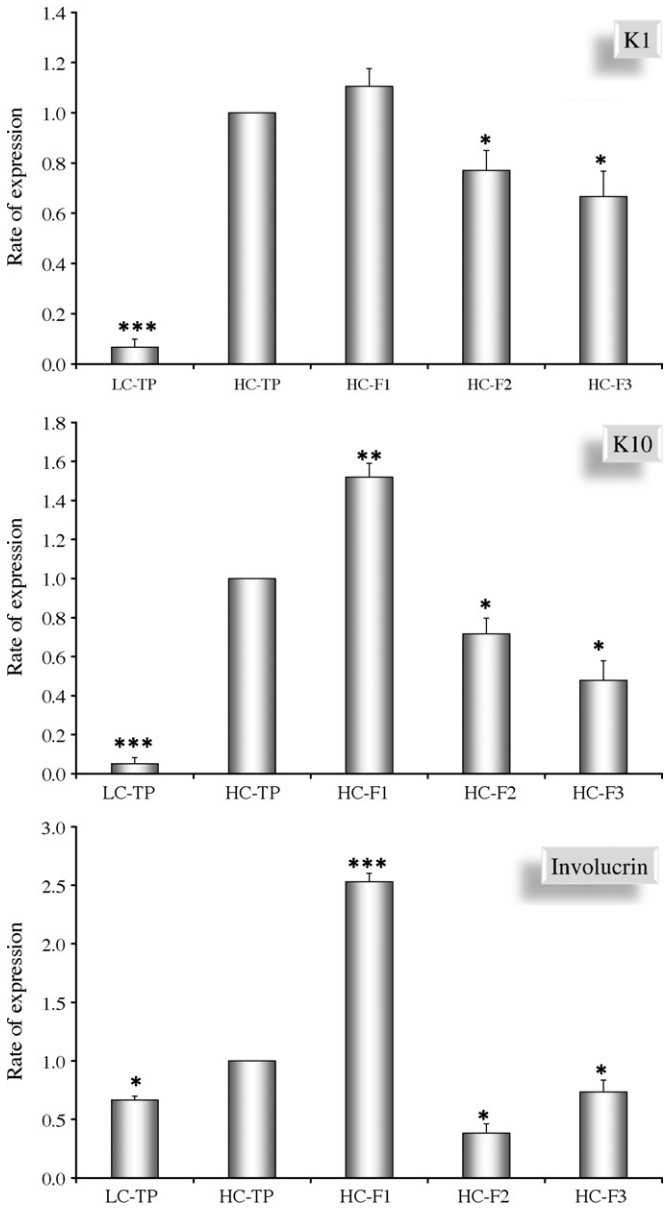

Fig. 3. Analysis of differentiation markers by semi-quantitative RT-PCR. K1, K10 and involucrin expression in HaCaT cells cultured in low (0.09 mM) or high (1.2 mM) extracellular calcium concentrations during 7 days and after SdFFF. For each marker, mRNA levels were normalized with a house keeping gene, as described in Section 2, and expressed in fold *vs.* the HC-TP value. Values represent means of three independent experiments respectively for HaCaT cells ± SD as described in Section 2. Asterisks correspond to *p*-values of LC TP, HC-F1, HC-F2 and HC-F3 *vs.* HC TP. $^{*}p < 0.05$; $^{**}p < 0.01$; $^{***}p < 0.001$.

than in HC-TP. In this context, SdFFF clearly focused differentiated cells in HC-F1, characterized by the strongest expression of differentiation markers K1, K10 and involucrin (Fig. 3).

3.3. Proliferative activity assay

To evaluate proliferative activity of HaCaT cells after SdFFF fractionation, the MTT colorimetric assay was performed as described in the literature [50]. After SdFFF fractionation, each cell sample was counted by the trypan blue dye exclusion method. Then, cell samples were seeded at the same density to compare proliferative activity at 24, 72 and 96 h post-seeding (Fig. 4).

For TP fractions, the higher proliferative activity of HC cells, in comparison to LC cells [14], was confirmed and conserved after

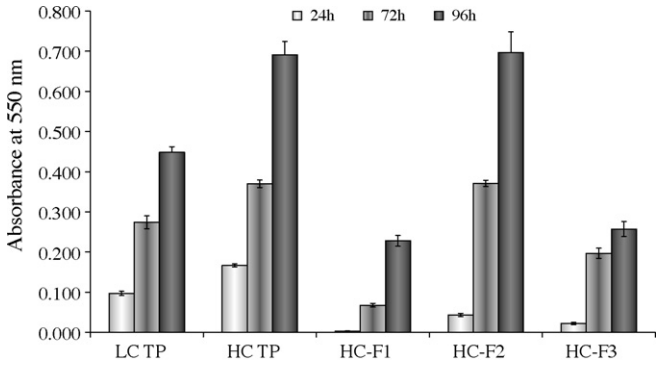

Fig. 4. Proliferative activity of HaCaT cells after SdFFF sorting in high (HC-TP, F1, F2 and F3) and low (LC-TP) calcium-containing medium. Graph depicts proliferative activity in which each cell sample was plated at the same density (3×10^3 cells/cm^2) and proliferative activity (Abs_{550}) was assessed by MTT assay 24, 72 and 96 h post-seeding. Values represent mean ± SD of three independent cell culture experiments.

SdFFF sorting. Cells in HC-F2 grew similarly to HC-TP, demonstrating that this fraction contained cells responsible for HC cell proliferation (Fig. 4). This was not the case for HC-F1 for which no proliferative activity was detected after 24 h. Despite an increase started at 72 h, HC-F1 proliferative activity was clearly delayed compared to F2. Finally, it appeared that HC-F3 cells had an intermediate profile, characterized by an increased proliferative activity between 24 and 72 h, but not between 72 and 96 h.

3.4. Analysis of DNA content by flow cytometry

In contrast to LC, HC cultured HaCaT cells were mainly distributed in the S/G2-M phases of the cell cycle, which correlated with their higher proliferative activity [14]. As it had been shown that SdFFF could separate cells according to cell cycle distribution [48], we determined whether or not fractionation was correlated with cell cycle distribution (Fig. 5). Results obtained for LC-TP and HC-TP were similar to those observed previously: (1) LC cells were mainly in G0/G1, due in part to confluence, which induced differentiation [12,13,15]; (2) whereas HC cells accumulated in S/G2-M [14]. The cell cycle profile of HC-F2 (Fig. 5) was similar to HC-TP: cells were mainly distributed in S/G2-M, in contrast to F3, where cells were mainly in G0/G1 (Fig. 5). These results showed that differences in proliferation between HC-F2 and HC-F3 were intrinsically correlated with cell cycle position. Here, HC-F3 cells had a lower rate of proliferation than HC-F2 and were mainly in G0/G1. Gen-

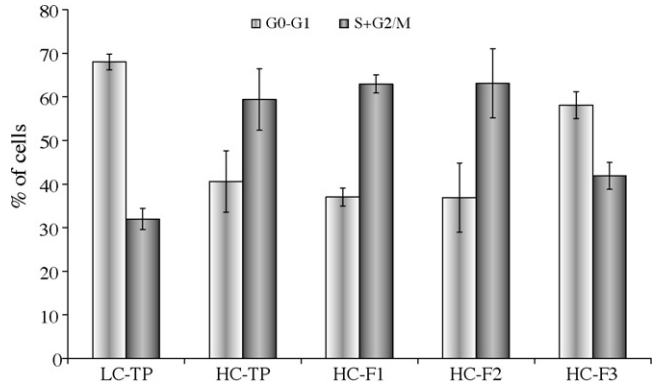

Fig. 5. Cell cycle distribution in HaCaT cells after SdFFF sorting. Cells were cultured in LC (0.09 mM Ca^{2+}) or HC (1.2 mM Ca^{2+}) medium for 7 days. Cell cycle distribution was determined by PI staining and FACS analysis as described in Section 2. Data are expressed as the mean ± SD of three independent experiments.

erally, cells in G0/G1 were smaller than cells in S/G2-M, and were eluted later by SdFFF [48]. Interestingly, HC-F1 cells, which predominantly expressed differentiation markers (K1, K10, involucrin) in correlation with the lowest proliferative activity, were mainly in S/G2-M (Fig. 5). More than likely their cell cycle would be arrested at this stage. Although this result appeared to be in good agreement with those previously obtained for HC cells [14], further studies are needed to validate this hypothesis.

The HaCaT cell line is routinely used as a human keratinocyte model *in vitro*. Like NHKs, HaCaT differentiation is induced either with confluence, when cells are cultured in a calcium free medium [12–15] or with Ca^{2+} concentrations superior to 1 mM [62,63]. In both cell types, Ca^{2+}-induced differentiation is observed by an increased expression of differentiation markers, such as K1, K10 and involucrin [5–10]. In NHKs, K1, K10 and involucrin expression significantly increased from the first day after Ca^{2+} addition. On the other hand, in the same conditions, increased differentiation markers in HaCaT cells are delayed: K1 and K10 increase after 3 days, and involucrin increases only 6 days after Ca^{2+} addition [14]. Surprisingly, Ca^{2+} leads to an increase in HaCaT proliferation, in contrast to NHKs [14]. These results led to many questions, in particular concerning the emergence throughout the differentiation process of subpopulations having different differentiation states and proliferation kinetics. We used SdFFF in order to sort cells as a function of proliferative activity and differentiation stage. SdFFF allowed the "Hyperlayer" elution of both LC and HC cells. SdFFF takes into account the change in size/density balance induced by Ca^{2+}. HC and LC cells displayed different size selectivity (S_{dObs}) values, due to the increased size of HC-F1 cells, while HC and LC cells eluted in F2 and F3 behaved similarly. These biophysical changes were closely correlated with biological processes. HC-F1 cells expressed the highest levels of K1, K10 and involucrin compared to HC-F2/-F3 or LC cells. These differentiated cells appeared to be blocked in S/G2-M, which was in agreement with previous results obtained from the total HC population [14]. This accumulation was linked to a large decrease in proliferative activity, in particular at 24 or 48 h post-seeding. In contrast, HC-F2 cells, less differentiated cells, showed the highest rate of proliferation, which was in agreement with their cell cycle position (S/G2-M), as cells with high proliferative activity undergo mitosis. Finally, HC-F3 cells appeared to be the least differentiated and least proliferative cells due to their quiescent state (G0/G1 cell cycle position).

4. Conclusion

With the aim of understanding why HaCaT cells conserved high rate of proliferation despite Ca^{2+}-induced differentiation characterized by increased differentiation marker expression [14], we tried to demonstrate the existence of several sub-cellular populations during Ca^{2+}-induced differentiation of HaCaT cells. By using the "Hyperlayer" SdFFF cell sorting method, which takes into account variations of the size/density balance occurring throughout differentiation, we were able to isolate subpopulations as a function of differentiation stages and proliferation rate.

Taken together, results demonstrated that HC-F1 cells which were the most differentiated cells, with increased expression of keratinocyte differentiation markers, had the lowest proliferative activity. This result was in good agreement with the classical description of differentiated cells which stop proliferating. In contrast, less HC differentiated cells had a greater proliferative activity than that observed in the LC population. By using SdFFF, we have a tool to sort differentiated and proliferating cells, allowing preparation of biological models for future studies in order to investigate how high Ca^{2+} levels increase proliferation of less differentiated cells in the HC population.

Acknowledgements

Authors are grateful to Dr. C. Jayat-Vignoles (Service Commun de Cytométrie, Université de Limoges) for valuable advice concerning flow cytometry analysis. The expenses of this work were defrayed in part by the Ministère de l'Education Nationale, de la Recherche et de la Technologie, the Conseil Régional du Limousin and by the Ligue contre le Cancer (Comité du Limousin).

References

[1] S.T. Boyce, R.G. Ham, J. Invest. Dermatol. 81 (1983) 33s.
[2] C. Missero, C.F. Di, H. Kiyokawa, A. Koff, G.P. Dotto, Genes Dev. 10 (1996) 3065.
[3] J.E. Lewis, P.J. Jensen, M.J. Wheelock, J. Invest. Dermatol. 102 (1994) 870.
[4] F.M. Watt, D.L. Mattey, D.R. Garrod, J. Cell Biol. 99 (1984) 2211.
[5] E. Fuchs, J. Cell Sci. Suppl. 17 (1993) 197.
[6] J. Woodcock-Mitchell, R. Eichner, W.G. Nelson, T.T. Sun, J. Cell Biol. 95 (1982) 580.
[7] R.M. Porter, E.B. Lane, Trends Genet. 19 (2003) 278.
[8] R.H. Rice, H. Green, Cell Biophys. 18 (1979) 681.
[9] R.L. Eckert, H. Green, Cell Biophys. 46 (1986) 583.
[10] E. Fuchs, J. Cell Biol. 111 (1990) 2807.
[11] P. Boukamp, R.T. Petrussevska, D. Breitkreutz, J. Hornung, A. Markham, N.E. Fusenig, J. Cell Biol. 106 (1988) 761.
[12] O. Garach-Jehoshua, A. Ravid, U.A. Liberman, J. Reichrath, T. Glaser, R. Koren, Br. J. Dermatol. 139 (1998) 950.
[13] M. Kato, A. Ishizaki, U. Hellman, C. Wernstedt, M. Kyogoku, K. Miyazono, C.H.F.K. Heldin, J. Biol. Chem. 270 (1995) 12373.
[14] L. Micallef, F. Belaubre, A. Pinon, C. Jayat-Vignoles, C. Delage, M. Charveron, A. Simon, Exp. Dermatol. 18 (2008) 143.
[15] C.M. Ryle, D. Breitkreutz, H.J. Stark, I.M. Leigh, P.M. Steinert, D. Roop, N.E. Fusenig, Differentiation 40 (1989) 42.
[16] D. Walker, T. Sun, S. MacNeil, R. Smallwood, Tissue Eng. 12 (2006) 2301.
[17] S. Battu, J. Cook-Moreau, P.J.P. Cardot, J. Liq. Chromatogr. Relat. Technol. 25 (2002) 2193.
[18] P. Reschiglian, A. Zattoni, B. Roda, E. Michelini, A. Roda, Trends Biotechnol. 23 (2005) 475.
[19] T. Kowalkowski, B. Buszewski, C. Cantado, F. Dondi, Crit. Rev. Anal. Chem. 36 (2006) 129.
[20] J. Bauer, J. Chromatogr. B 722 (1999) 55.
[21] D. Mattanovich, N. Borth, Microb. Cell Fact. 5 (2006) 1.
[22] M. Radisic, R.K. Lyer, S.K. Murthy, Int. J. Nanomed. 1 (2006) 3.
[23] D. Pappas, K. Wang, Anal. Chim. Acta 601 (2007) 26.
[24] Pethig, Lee, Talary, J. Assoc. Lab. Autom. 9 (2004) 324.
[25] M.A. McClain, C.T. Culbertson, S.C. Jacobson, N.L. Allbritton, C.E. Sims, J.M. Ramsey, Anal. Chem. 75 (2003) 5646.
[26] J.C. Giddings, Sep. Sci. 1 (1966) 123.
[27] J.C. Giddings, Science 260 (1993) 1456.
[28] T. Chianea, N.E. Assidjo, P.J.P. Cardot, Talanta 51 (2000) 835.
[29] K.D. Caldwell, Z.Q. Cheng, P. Hradecky, J.C. Giddings, Cell Biophys. 6 (1984) 233.
[30] J. Vykoukal, D.M. Vykoukal, S. Freyberg, E.U. Alt, P.R.C. Gascoyne, Lab on a Chip 8 (2008) 1386.
[31] B. Roda, P. Reschiglian, A. Zattoni, P.L. Tazzari, M. Buzzi, F. Ricci, A. Bontadini, Anal. Bioanal. Chem. 392 (2008) 137.
[32] P. Reschiglian, M.H. Moon, J. Proteomics 71 (2008) 265.
[33] D.I. Lipin, Y.P. Chuan, L.H.L. Lua, A.P.J. Middelberg, Arch. Virol. 153 (2008) 2027.
[34] D. Kang, S. Oh, S.-M. Ahn, B.-H. Lee, M.H. Moon, J. Proteome Res. 7 (2008) 3475.
[35] C. Arfvidsson, G. Wahlund Karl, Anal. Biochem. 313 (2003) 76.
[36] S. Battu, W. Elyaman, J. Hugon, P.J.P. Cardot, Biochim. Biophys. Acta 1528 (2001) 89.
[37] L. Farmakis, A. Koliadima, Biotechnol. Prog. ACS ASAP (2005).
[38] Y. Huang, J. Yang, X.B. Wang, F.F. Becker, P.R. Gascoyne, J. Hemathoth. Stem Cell 8 (1999) 481.
[39] J. Luo, M. Leeman, A. Ballagi, A. Elfwing, Z. Su, J.-C. Janson, K.-G. Wahlund, J. Chromatogr. A 1120 (2006) 158.
[40] C. Corbière, S. Battu, B. Liagre, P.J.P. Cardot, J.L. Beneytout, J. Chromatogr. B 808 (2004) 255.
[41] D.Y. Leger, S. Battu, B. Liagre, J.L. Beneytout, P.J.P. Cardot, Anal. Biochem. 355 (2006) 19.
[42] D.Y. Leger, B. Liagre, P.J.P. Cardot, J.L. Beneytout, S. Battu, Anal. Biochem. 335 (2004) 267.
[43] G. Bégaud-Grimaud, S. Battu, B. Liagre, D.Y. Léger, J.L. Beneytout, P.J.P. Cardot, J. Chromatogr. A 1128 (2006) 194.
[44] D.Y. Leger, S. Battu, B. Liagre, P.J.P. Cardot, J.L. Beneytout, J. Chromatogr. A 1157 (2007) 309.
[45] J. Bertrand, B. Liagre, G. Bégaud-Grimaud, M.O. Jauberteau, P. Cardot, J.L. Beneytout, S. Battu, J. Chromatogr. B 869 (2008) 75.
[46] G. Bégaud-Grimaud, S. Battu, P. Lazcoz, J.S. Castresana, M.O. Jauberteau, P.J.P. Cardot, Int. J. Oncol. 31 (2007) 883.
[47] C. Lautrette, P.J.P. Cardot, C. Vermot-Desroche, J. Wijdenes, M.O. Jauberteau, S. Battu, J. Chromatogr. B 791 (2003) 149.
[48] J. Bertrand, B. Liagre, G. Bégaud-Grimaud, M.O. Jauberteau, J.L. Beneytout, P.J.P. Cardot, S. Battu, J. Chromatogr. B 877 (2009) 1155.

[49] J. Vandesompele, P.K. De, F. Pattyn, B. Poppe, R.N. Van, P.A. De, F. Speleman, Genome Biol. 3 (2002) (research 0034.1).
[50] T. Mosmann, J. Immunol. Methods 65 (1983) 55.
[51] P.O. Harmand, R. Duval, B. Liagre, C. Jayat-Vignoles, J.L. Beneytout, C. Delage, A. Simon, Int. J. Oncol. 23 (2003) 105.
[52] L. Guglielmi, S. Battu, M. Le Bert, J.L. Faucher, P.J.P. Cardot, Y. Denizot, Anal. Chem. 76 (2004) 1580.
[53] J. Chmelik, J. Chromatogr. A 845 (1999) 285.
[54] M. Martin, P.S. Williams, in: F. Dondi, G. Guiochon (Eds.), Theoretical Advancement in Chromatography and Related Separation Techniques, Kluwer, Dordrecht, 1992, p. 513.
[55] M.R. Schure, K.D. Caldwell, J.C. Giddings, Anal. Chem. 58 (1986) 1509.
[56] X. Tong, K.D. Caldwell, J. Chromatogr. B 674 (1995) 39.
[57] P.S. Williams, S. Lee, J.C. Giddings, Chem. Eng. Commun. 130 (1994) 143.
[58] P.S. Williams, J.C. Giddings, Anal. Chem. 66 (1994) 4215.
[59] C. Cailleteau, B. Liagre, S. Battu, C. Jayat-Vignoles, J.L. Beneytout, Anal. Biochem. 380 (2008) 26.
[60] R. Sanz, P. Cardot, S. Battu, M.T. Galceran, Anal. Chem. 74 (2002) 4496.
[61] M.E. Schimpf, in: M.E. Schimpf, K.D. Caldwell, J.C. Giddings (Eds.), Field-Flow Fractionation handbook, John Wiley & Sons, Inc., New York, 2000, p. 71.
[62] O. Pleguezuelos, S. Kapas, Br. J. Dermatol. 154 (2006) 602.
[63] E.Y. Seo, Y.J. Piao, J.S. Kim, K.B. Suhr, J.K. Park, J.H. Lee, Arch. Dermatol. Res. 294 (2002) 411.